MGSA-Type Computer-Generated Holography for Vision Training With Head-Mounted Display

Qing-Long Deng, Bor-Shyh Lin, Hsuan T. Chang, *Senior Member, IEEE*, Guan-Syun Huang, and Chien-Yue Chen

***Abstract*—A computer-generated holography head-mounted display (HMD) for vision training is proposed in this study. Based on modified Gerchberg–Saxton algorithm (MGSA) to calculate the phase distribution of light wave and the position multiplexing, the images with fixation disparity or changed disparity are successfully coded as phase only function. After decryption and reconstruction, the left and the right images are transmitted to HMD for a trainee viewing the images with disparity changes and moderating the stereoacuity of both eyes, ranging from 32.24 arcsec to 2.14 arcmin. The images reconstructed with MGSA-type CGH present the relative diffraction efficiency about 86% and visibility 94%, which not only provide high-contrast image quality, and the changing disparity allows achieving the training effect.**

***Index Terms*—Computer-generated holography, head-mounted display (HMD), stereo vision.**

I. Introduction

ACCOMMODATIVE convergence is an oculomotor cue of human vision. It describes that the ciliary muscle presents the focus function by adjusting the dioptre of crystalline lens and elicits the extraocular muscle for eye vergence when viewing an object. After completing the synkinesis of accommodation and convergence, the disparity of the target is acquired for the brain identifying the cues in depth [1]. The tension of ciliary muscle would decrease with the age increase and the flexibility of crystalline lens gets hardened so that the eyes could not clearly focus on the retinal when viewing close objects. Although the vergence strength of eyes could increase, the insufficient accommodation could still cause presbyopia [2].

Presently, femtosecond laser is used for changing the cornea curvature to increase the focus on close objects [3]; in recent years, vision trainings are applied to training eye muscles and reinforce the connection between the ciliary muscle and nerves.

Manuscript received April 01, 2013; revised June 05, 2013; accepted July 26, 2013. Date of publication August 07, 2013; date of current version May 05, 2014. This work is supported by the National Science Council of Taiwan under Contract NSC 101-2628-E-224-002-MY3.

Q.-L. Deng is with the Institute of Photonic Systems, National Chiao Tung University, Tainan 71150, Taiwan (e-mail: parite.deng@gmail.com).

B.-S. Lin is with the Institute of Imaging and Biomedical Photonics, National Chiao Tung University, Tainan 71150, Taiwan (e-mail: borshyhlin@gmail.com).

H. T. Chang is with the the Department of Electrical Engineering, National Yunlin University of Science and Technology, Douliou, Yunlin 64002, Taiwan (e-mail: htchang@yuntech.edu.tw).

G.-S. Huang is with the Graduate School of Electronic and Optoelectronic Engineering, National Yunlin University of Science and Technology, Douliou, Yunlin 64002, Taiwan (e-mail: m10013333@yuntech.edu.tw).

C.-Y. Chen is with the Department of Electronics Engineering, National Yunlin University of Science and Technology, Douliou, Yunlin, 64002, Taiwan (e-mail: chencyue@ yuntech.edu.tw).

Color versions of one or more of the figures are available online at http://ieeexplore.ieee.org.

Digital Object Identifier 10.1109/JDT.2013.2276129

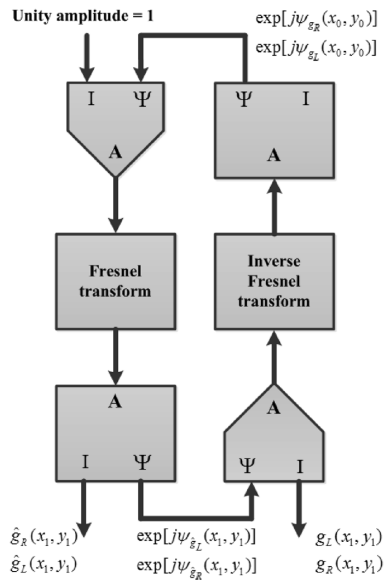

Fig. 1. MGSA computing flow chart.

Although it would spend longer time for improvement, it could avoid relevant medical risks; besides, trainings in pre-presbyopia could make more effective improvement [4]–[6]. General vision trainings have the trainees view the left and the right picture cards with distinct distances and try to cross fuse the two images with focus as cyclopean vision [7]. Nonetheless, it might be difficult for the trainees recognizing the images with low contrast and blurred characterized images.

For this reason, an applied computer generated holography based on the modified Gerchberg–Saxton algorithm [8] to calculate the phase distribution of light wave and position multiplexing is proposed in this study. The parallax content of a stereoscopic image is keyed in the head-mounted display for vision training. In this study, MGSA-type CGH is utilized for calculating the image contents of fixation disparity and changed disparity so that the trainees could train the modulation of ciliary muscle and the convergence through fixation disparity and changed disparity, respectively.

II. Methods

A. Principle of Modified Gerchberg-Saxton Algorithm (MGSA)

The modified Gerchberg–Saxton algorithm (MGSA) is utilized in this study for rapidly calculating the complete phase wave function, where Fresnel transform (FrT) (1) is used for repeatedly iterating the phase between objects to modify the phase difference [8], [9]. Different from traditional Gerchberg–Saxton algorithm [10], it could enhance the computing speed. The MGSA flow chart is shown in Fig. 1.

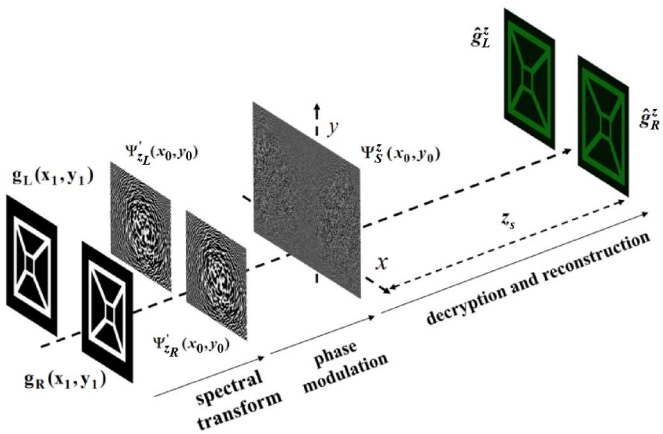

Fig. 2. MGSA-type CGH coding and decryption.

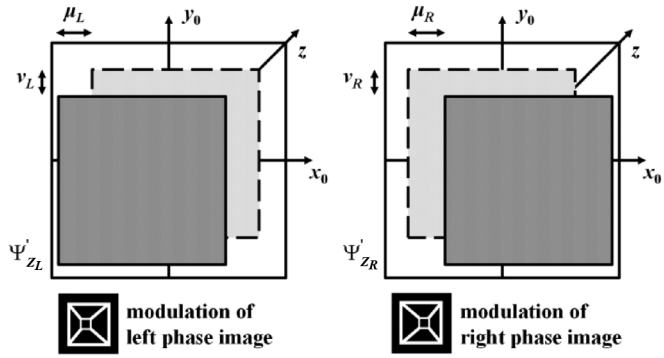

Fig. 3. Modulation diagram of spatial phase.

First, two random phase functions $\psi_{g_L}(x_0, y_0)$ and $\psi_{g_R}(x_0, y_0)$ are input, and then the initially set amplitude and step phase function $\exp[j\psi_{g_R}(x_0, y_0)]$ and $\exp[j\psi_{g_L}(x_0, y_0)]$ are multiplied by Fresnel transform. The amplitude $\hat{g}_R(x_1, y_1)$ and $\hat{g}_L(x_1, y_1)$ and phases $\psi_{\hat{g}_L}(x_1, y_1)$ and $\psi_{\hat{g}_R}(x_1, y_1)$ are then acquired. The original images $g_R(x_1, y_1)$ and $g_L(x_1, y_1)$ and the update phase $\exp[j\psi_{\hat{g}_L}(x_1, y_1)]$ and $\exp[j\psi_{\hat{g}_R}(x_1, y_1)]$ are proceeded inverse Fresnel transform. The loop steps are repeated till the estimated images $\hat{g}_R(x_1, y_1)$ and $\hat{g}_L(x_1, y_1)$ close to the thresholds of the originally input images $g_R(x_1, y_1)$ and $g_L(x_1, y_1)$. The coded map with same phase and amplitude as the original images is then completed, called phase only function (POF). Equations (2) and (3) show the image Fresnel diffraction transforming to MGSA equation and the relevant coefficients

$$E(x,y,z) = \frac{\exp\left(\frac{j2\pi z}{\lambda}\right)}{j\lambda z} \exp\left[\frac{j\pi}{\lambda z}(x^2+y^2)\right] \times \mathrm{FrT}\left\{E(x',y',0)\exp\left[\frac{j\pi}{\lambda z}(x'^2+y'^2)\right]\right\}, \quad p = \left(\frac{x}{\lambda z}\right); q = \left(\frac{y}{\lambda z}\right) \tag{1}$$

where λ is the wavelength of incident light, $E(x, y, z)$ is the coordinate of original image, $E(x', y', 0)$ is the diffraction imaging coordinate of original image plane through FrT, z is the distance between the original image plane and the diffraction imaging plane, p is the spatial frequency in x-direction, and q is the spatial frequency in z-direction

$$\mathrm{FrT}\left\{\exp\left[j\psi_{z_L}(x_0,y_0)\right];\lambda;z_{S1}\right\} = \hat{g}_L^z(x_1,y_1)\exp\left[j\psi_{\hat{g}_L}^z(x_1,y_1)\right] \tag{2}$$

$$\mathrm{FrT}\left\{\exp\left[j\psi_{z_R}(x_0,y_0)\right];\lambda;z_{S2}\right\} = \hat{g}_R^z(x_1,y_1)\exp\left[j\psi_{\hat{g}_R}^z(x_1,y_1)\right]. \tag{3}$$

B. Spatial Phase Modulation and Synthesis

Fig. 2 shows the coding and decryption of MGSA-type CGH. After MGSA spectral conversion, the left and the right images merely present POF with amplitude and phase, where each pixel stands for the grating interfered by each object light and the reference light and the original image data are decrypted. Nonetheless, the multicomplexing algorithm in spatial phase modulation (4) is applied to recording the image information in the same POF, as shown in Fig. 3.

The light gray areas in the figure are the originally coded POF. After spatial phase modulation, the diffraction spatial distribution is changed to transform the target image to different space locations (dark gray areas) and complete position multiplexing distribution (where the modulation of left image is shown by (5) and (6); the modulation of right image is shown by (7) and (8)). When POF is decrypted through photo-reconstruction, all interference fields generated from grating are iterated so that the amplitude and phase of each pixel are modulated the light intensity and direction for reconstructing the original image content

$$A_S^z(x_0,y_0)\exp\left[j\psi_S^z(x_0,y_0)\right] = \exp\left[j\psi'_{z_L}(x_0,y_0)\right] + \exp\left[j\psi'_{z_R}(x_0,y_0)\right] \tag{4}$$

$$\mathrm{FrT}\left\{\exp\left[j\psi'_{z_L}(x_0,y_0)\right];\lambda;z_{S1}\right\} = \hat{g}_L^z(x_1-\mu_L, y_1-v_L)\exp\left[j\varphi_L(x_1,y_1)\right] \tag{5}$$

$$\psi'_{z_L}(x_0,y_0) = j\psi_{z_L}(x_0,y_0) + [2\pi(\mu_L x_0 + v_L y_0)/\lambda z_{S1}] \tag{6}$$

$$\mathrm{FrT}\left\{\exp\left[j\psi'_{z_R}(x_0,y_0)\right];\lambda;z_{S2}\right\} = \hat{g}_R^z(x_1-\mu_R, y_1-v_R)\exp\left[j\varphi_R(x_1,y_1)\right] \tag{7}$$

$$\psi'_{z_R}(x_0,y_0) = j\psi_{z_R}(x_0,y_0) + [2\pi(\mu_R x_0 + v_R y_0)/\lambda z_{S2}] \tag{8}$$

where $A_S^z(x_0, y_0)$ and $\exp[j\psi_S^z(x_0, y_0)]$ are the summed amplitude and phase synthesis of output signals, $\hat{g}_L^z(x_1, y_1)$ and $\hat{g}_R^z(x_1, y_1)$ are the reconstructed images in the diffraction space, μ_L and μ_R are the offset distance in x direction, v_L and v_R are the offset distance in y direction, $\varphi_R(x_1, y_1)$ and $\varphi_L(x_1, y_1)$ are the phase items of images reconstructed by phase signals $\psi'_{z_L}(x_0, y_0)$ and $\psi'_{z_R}(x_0, y_0)$, which are modulated from the initial phase, through Fresnel transform.

C. Binocular Stereogram

In the binocular stereogram, the disparity determines the synkines is of accommodation and convergence, accommodative convergence (AC) could be induced by fixation disparity, and convergence accommodation (CA) is induced by changed disparity.

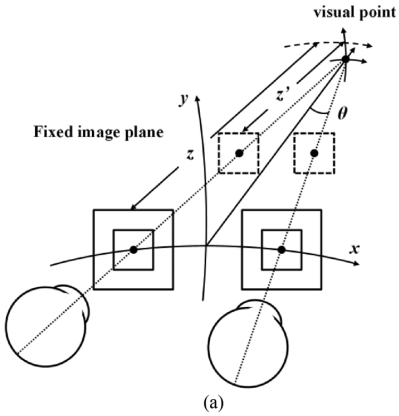

(a)

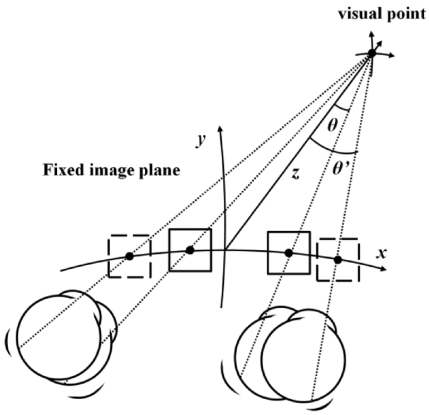

(b)

Fig. 4. (a). Diagram of binocular vision with fixation disparity. (z is the distance between large pattern, z' is the distance between small pattern, θ is the stereoacuity). (b). Diagram of binocular vision with changed disparity. (z is the distance from the fixed image plane to the visual point, θ is the stereoacuity of the small disparity pattern [solid line), θ' is the stereoacuity of the large disparity pattern (dotted line).]

Fixation disparity is defined as the characterized image whose left and right sizes are different but present same disparity, as shown in Fig. 4(a). In the figure, when the characterized image with fixation disparity is located on the fixed image plane, it is regarded as the image projected from different distances. In other words, when both eyes viewing the left and the right images with the same disparity, the perception disorder is caused by the distinct sizes. The ciliary muscle therefore appears indirect accommodation because of monocular cues to complete fusional convergence [11], [12].

On the contrary, Fig. 4(b) shows the changed disparity which is defined as the left and the right characterized images with the same size but changeable disparity. It aims to change the eyes' vergence through the characterized image with distinct disparity for inducing the accommodation change.

As a result, the above MGSA-type CGH is applied to coding image contents with fixation disparity and changed disparity for vision trainings.

III. Experiment and Analysis

Fig. 5 illustrates a prototype of MGSA-type CGH system with head-mounted display (HMD) for vision trainings. First, the DPSS laser (532 nm) is used for decrypting the coherence of light, which is adjusted to proper intensity with neutral density filters and then injected to the spatial light modulation

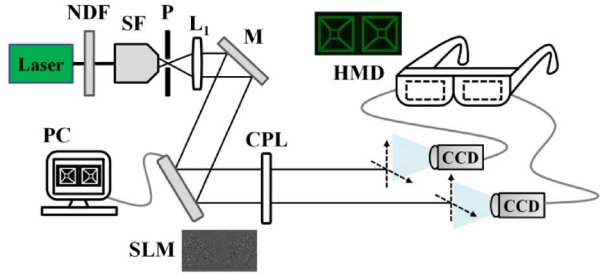

Fig. 5. Diagram of prototype MGSA-type CGH system with HMD. (L_1 represents lens, NDF represents neutral density filters, SF represents spatial filter, P represents pinhole, M represents mirror, CPL represents circular polarizer lens, spatial light modulator is denoted SLM, and the HMD is labeled HMD.)

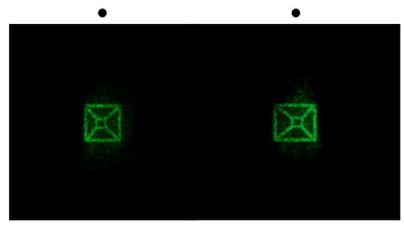

Fig. 6. Stereo image pair with the changed disparity.

(WUXGA, 8.1 μm, HOLOEYE) through the collimating lens. SLM records POF with fixation disparity or changed disparity coded by MGSA. After the decryption, the image reconstructed by diffraction light is projected to CCD and transmitted to the head-mounted display for the trainee proceeding vision trainings through HMD. Fig. 6 shows a changed disparity image which is transmitted to HMD after the decryption. With cyclopean vision [7], the stereo image in the figure would extrude the screen when the dot viewed by both eyes would be convergent to a point.

A. Analysis of Reconstruction Image

In addition to calculating the image contents with fixation disparity and changed disparity by MGSA, each pixel is multiplied by random number phase when being computed and proceeded Fresnel transform to improve the noise caused by amplified low-frequency signals during spectral matrix computation for maintaining the reconstructed image quality after the decryption.

To effectively acquire the image quality of POF after the decryption, a computer computation is first utilized for evaluating the decrypted image with the following methods from (9) to (11). 1) The relative diffraction efficiency is defined as the intensity proportion of the zeroth-order diffraction light in the incident light in the signal area. 2) The root mean square error (RMSE) is defined as the difference between the original image and the reconstructed image of each pixel. 3) The signal-to-noise ratio (SNR) is defined as the ratio of signal power and noise power. 4) The computation average time is the computation speed for coding POF. The decrypted image is further analyzed, where visibility [13] and speckle [14] are also analyzed by using (12) and (13), the results are shown in Table I.

From the table, both the images decrypted by computer computation or reconstructing light appear RMSE lower than 0.05, showing that POF coded by MGSA could acquire the content as

TABLE I
SIMULATION AND ANALYSES OF RECONSTRUCTED IMAGES

	Calculation		Experiment	
	Left	Right	Left	Right
I_{max} (μW/mm^2)	n/a	n/a	53.45	52.63
I_{min} (μW/mm^2)	n/a	n/a	1.68	1.50
Visibility (%)	n/a	n/a	94.07	94.46
Diffraction efficiency (%)	96.58	96.78	87.49	86.26
RMSE	0.03	0.03	0.04	0.04
SNR (dB)	14.51	14.78	8.44	7.94
Speckle contrast (%)	n/a		20.23	

the original image after the decryption. Moreover, in regard to the evaluation of diffraction efficiency, the decryption efficiency (∼85%) is slightly lower than the result of computer computation (∼95%), but the image intensity can be accepted by human eyes.

What is more, the reconstructed left and right images reveal the visibility 94.07% and 94.46%, respectively, showing the characteristic line of the decrypted image with favorable contrast, that the content could be clearly presented. Besides, the SNRs appear 8.44 dB and 7.94 dB, and the speckle is 20.23% after the random number phase multiplication that the noise disturbance has been reduced about a half, compared to traditional CGH [15]. Moreover, the computation average time is 60.28 s, revealing that the same or better image quality could be achieved by faster computation speed and less number of iteration times, compared to general holographic projection systems [15]–[17]

$$I_{\mathrm{DE}} = \sum_S I_S \Big/ \left(\sum_S I_S - \sum_N I_N \right) \times 100\% \quad (9)$$

$$\mathrm{RMSE} = \sqrt{\left(\frac{\sum I_N^2}{MN} \right)} \quad (10)$$

$$\mathrm{SNR} = 10 \times \log_{10} \left(\frac{I_S}{I_N} \right) \quad (11)$$

$$\mathrm{visibility} = \frac{(I_{\max} - I_{\min})}{(I_{\max} + I_{\min})} \times 100\% \quad (12)$$

$$\mathrm{speckle\ contrast} = \frac{\sqrt{\langle I^2 \rangle - \langle I \rangle^2}}{\langle I \rangle} \times 100\% \quad (13)$$

B. Analysis of Stereogram

HMD in Fig. 5 is composed of two liquid crystal displays, with the virtual distance 2 m and the transverse magnification 12 times. A trainee receives two different reconstructed images (fixation disparity image or changed disparity image) and both eyes maintain accommodation to the LCD screen. Meanwhile, the physiological mechanism of extraocular muscle is induced for both eyes proceeding vergence. When the viewed image features are completed fusion, the stereoscopic depth of the image (crossed parallax or uncrossed parallax) is further judged [7], as shown in Fig. 7.

The SLM resolution is 1920 pixel × 1200 pixel that the disparity appears 7.78 mm after coding the fixation disparity image with MGSA, and the disparity of the reconstructed image on HMD shows 93.31 mm [see Fig. 7(a)]. In this case, when viewing the images through HMD, the stereoacuity of crossed parallax caused by fusion appears 1.33 arcmin (uncrossed parallax is 1.27 arcmin). Furthermore, the disparity of the reconstructed images in Fig. 7(b) is the same as it in Fig. 7(a), but illusion (the relationship between size and distance) would appear because of monocular cues that the brain would judge the image being farther. As a result, the accommodation would be indirectly changed to increase the stereoacuity.

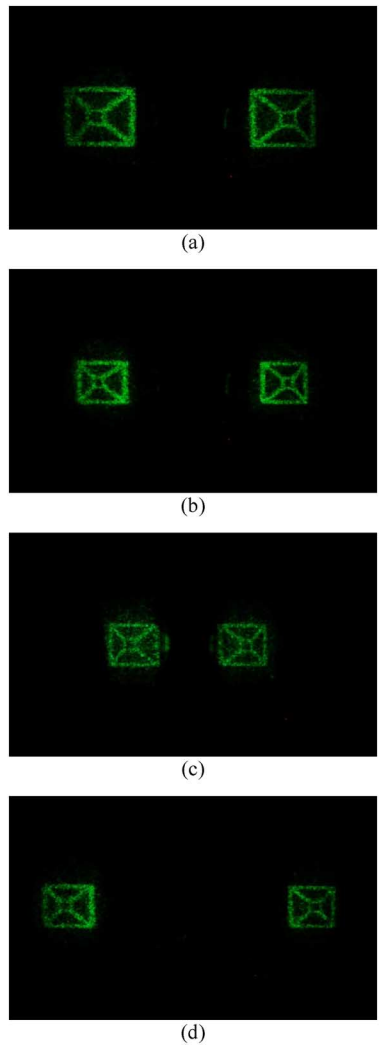

Fig. 7. Images with different disparity changes: (a) fixation disparity image 1; (b) fixation disparity image 2; (c) changed disparity image 1; and (d) changed disparity image 2.

In the changed disparity style, the decoded and reconstructed images show the same size of 38.88 mm×38.88 mm, and the disparity changes from 38.88 mm to 147.74 mm, as shown in Fig. 7(c) and 7(d). The stereoacuity in crossed parallax therefore changes from 32.91 arcsec to 2.14 arcmin, and the stereoacuity changes from 32.24 arcsec to 1.99 arcmin in uncrossed parallax.

In this case, having a trainee view such images with two different styles allows the accommodation and convergence of eyes influencing each other for vision training. It even corresponds to the maximal restriction of stereoacuity[18].

IV. Conclusion

The MGSA is used for the computer generated hologram coding of fixation disparity image or changed disparity image and the left and the right reconstructed image information is displayed on HMD. Such a method allows a trainee viewing the images with two different disparities through HMD and further changing the synkinesis of accommodation and convergence (the stereoacuity appears 32.24 arcsec to 2.14 arcmin) for effectively training ciliary muscle and extraocular muscle. Besides, the reconstructed images show the relative diffraction efficiency about 86% and visibility 94%. In comparison with traditional 2D cards, the images reconstructed by MGSA-type CGH present high contrast, high resolution, and changeable disparity that they could enhance the training effect and avoid crosstalk between the left and the right images.

References

[1] D. Kersten and G. E. Legge, "Convergence accommodation," *J. OSA*, vol. 73, pp. 332–338, 1983.

[2] A. S. Bruce, D. A. Atchison, and H. Bhoola, "Accommodation-convergence relationships and age," *Invest. Ophthalmol. Vis. Sci.*, vol. 36, no. 2, pp. 406–413, 1995.

[3] H. K. Soong and J. B. Malta, "Femtosecond lasers in ophthalmology," *Amer. J. Ophthalmol.*, vol. 147, pp. 189–197, 2009.

[4] J. Maxwell, J. Tong, and C. M. Schor, "Short-term adaptation of accommodation, accommodative vergence and disparity vergence facility," *Vision Res.*, vol. 62, pp. 93–101, 2012.

[5] J. Maxwell, J. Tong, and C. M. Schor, "The first and second order dynamics of accommodative convergence and disparity convergence," *Vision Res.*, vol. 50, pp. 1728–1739, 2010.

[6] U. Polat, "Making perceptual learning practical to improve visual functions," *Vision Res.*, vol. 49, pp. 2566–2573, 2009.

[7] B. Julesz, "Cyclopean perception and neurophysiology," *Invest. Ophthalmol. Vis. Sci.*, vol. 11, pp. 540–548, 1972.

[8] H. E. Hwang, H. T. Chang, and W. N. Lai, "Fast double-phase retrieval in Fresnel domain using modified Gerchberg–Saxton algorithm for lensless optical security systems," *Opt. Express*, vol. 17, pp. 13700–13710, Aug. 2009.

[9] H. E. Hwang, H. T. Chang, and W. N. Lie, "Multiple-image encryption and multiplexing using a modified Gerchberg-Saxton algorithm and phase modulation in Fresnel-transform domain," *Opt. Lett.*, vol. 34, pp. 3917–3919, 2009.

[10] R. W. Gerchberg and W. O. Saxton, "A practical algorithm for the determination of phase from image and diffraction plane pictures," *Optik*, vol. 35, pp. 237–246, 1972.

[11] J. M. Hillis and M. S. Banks, "Are corresponding points fixed?," *Vision Res.*, vol. 41, pp. 2457–2473, 2001.

[12] R. F. Fisher, "The force of contraction of the human ciliary muscle during accommodation," *J. Physiol.-London*, vol. 270, pp. 51–74, 1977.

[13] E. J. Seykora, "Solar interferometry utilizing the visibility of diffraction-free images," *Appl. Opt.*, vol. 29, pp. 5039–5041, 1990.

[14] C. Y. Chen, W. C. Su, C. H. Lin, M. D. Ke, Q. L. Deng, and K. Y. Chiu, "Reduction of speckles and distortion in projection system by using a rotating diffuser," *Opt. Rev.*, vol. 19, pp. 440–443, 2012.

[15] K. Choi, H. Kim, and B. Lee, "Synthetic phase holograms for autostereoscopic image display using a modified IFTA," *Opt. Express*, vol. 12, pp. 2454–2462, 2004.

[16] J. P. Liu, W. Y. Hsieh, T. C. Poon, and P. Tsang, "Complex Fresnel hologram display using a single SLM," *Appl. Opt.*, vol. 50, pp. H128–H135, 2011.

[17] J. Bu, G. Yuan, Y. Sun, S. Zhu, and X. Yuan, "Optimization of computer-generated holograms for dynamic optical manipulation with uniform structured light spots," *Chin. Opt. Lett.*, vol. 9, pp. 061202–, 2011.

[18] Y. Y. Yehand and L. D. Silverstein, "Limits of fusion and depth judgment in stereoscopic color displays," *Human Factors*, vol. 32, pp. 45–60, 1990.

Qing-Long Deng received the B.S. degree in electronical engineering in 2008, and the M.S. degree in optoelectronic engineering in 2010, both from National Yunlin University of Science and Technology, Taiwan, and is currently working toward the Ph.D. degree at Institute of Photonic Systems, National Chiao Tung University, Taiwan. His research interests include autostereoscopy, optical design and optical information processing.

Bor-Shyh Lin received the B.S. degree from National Chiao Tung University (NCTU), Taiwan, in 1997, and the M.S. and Ph.D. degrees in electrical engineering from National Taiwan University (NTU), Taiwan, in 1999 and 2006, respectively.

He is currently Assistant Professor of the Institute of Imaging and Biomedical Photonics, National Chiao Tung University (NCTU), Taiwan. His research interests are in the areas of Biomedical Circuits and Systems, Biomedical Signal Processing, and Biosensor.

Hsuan T. Chang (M'02–SM'06) received the B.S. degree in electronic engineering from National Taiwan University of Science and Technology, Taiwan, in 1991, and the M.S. and Ph.D. degrees in Electrical Engineering (EE) from National Chung Cheng University (NCCU), Taiwan, in 1993 and 1997, respectively.

From 2001 to 2002, he was an assistant professor and from 2003 to 2006, he was an associate professor in EE Department of National Yunlin University of Science and Technology (YunTech), Douliu, Taiwan. He currently is a full professor in EE Department of YunTech. His interests include image/video analysis, optical information processing/computing, medical image processing, and human computer interface. He has published more than 40 journal and 140 conference papers in the above research areas.

Dr. Chang is member of the Optical Society of America (OSA), and International Society for Optical Engineering (SPIE), member of Taiwanese Association of Consumer Electronics (TACE), Asia-Pacific Signal and Information Processing Association (APSIPA), and The Chinese Image Processing and Pattern Recognition (IPPR) Society.

Guan-Syun Huang received the B.S. degree in Department of Electronic Engineering from National Ilan University, Taiwan in 2011, and is currently working toward the M.S. degree in Optoelectronic Engineering from National Yunlin University of Science and Technology, Taiwan. His research interests include holography, optical design, and autostereoscopy.

Chien-Yue Chen was born in Taitung, Taiwan, 1969. He received the B.S. degree in physics from Soochow University in 1992, the M.S. degree and the Ph.D. degree in space science and optical science individually, from National Central University, Taiwan, in 1994 and 2004, respectively.

He is currently a professor at the Department of Electronics Engineering, National Yunlin University of Science and Technology, Taiwan. His research interests include optical design, micro-optics and 3D technology.